

Application of Optimal GNSS Multi-Frequency Carrier Phase Combinations to Kinematic Positioning

Todd Richert
Mobile Multi-Sensor Research Group
Geomatics Engineering Department
University of Calgary
Calgary, Canada
taricher@ucalgary.ca

Co-Authors:

Dr. Robert Radovanovic, SARPI Ltd., Calgary, Canada, solutions@sarpigroup.com

Dr. Naser El-Sheimy, Mobile Multi-Sensor Research Group, Geomatics Engineering Department, University of Calgary, Canada, naser@geomatics.ucalgary.ca

1 Abstract

As the number of ranging observations available increases with the development of new Global Navigation Satellite Systems, and as frequencies are added to existing systems such as the Global Positioning System, bandwidth constraints become an issue when the transmission and processing of multi-frequency data is required for kinematic network processing. One method of limiting the amount of data that needs to be transmitted and processed is via the compression of multi-frequency data into a single pseudo-observation through a linear phase combination.

Traditional combinations of dual-frequency GPS carrier phase data have focused on three combinations, namely the widelane, the narrowlane, and the ionosphere-free combination. All of these combinations suffer from limitations, which affect the overall accuracy of precise positioning. The disadvantage of the ionosphere-free combination is that the resolved ambiguities are not integer; the disadvantage of using the widelane combination is that the resulting positioning accuracy is degraded from the inherent amplification of noise; and the disadvantage of the narrowlane combination is that it is very difficult to resolve the correct ambiguity values. Furthermore, previous studies of phase combinations have regarded errors on both frequencies as independent. In reality, errors such as tropospheric and ionospheric delays are correlated between frequencies. Thus, combinations of phase

measurements may actually have reduced error magnitudes compared to the original measurements.

This paper presents the results of applying the concept of linear phase combinations to high precision kinematic positioning. To gauge the utility of the linear phase combinations, simulation data as well as two sets of test data are processed using various data combinations. It is found in this study that for a five kilometer baseline, the combination described by $\Phi_* = 2\Phi_{L1} - \Phi_{L2}$ optimizes the achievable positioning accuracy. The position accuracy attained is better than that of using the pure L1 signal and an adequate level of reliability in terms of fixing the correct integer ambiguities is maintained. Choosing an optimal combination of signals for a specific application depends on the spatial extent of the network and on the specific GPS positioning environment.

2 Introduction

For multi-receiver GPS networks used in real-time applications, there is a need to reduce the quantity of data to be transmitted from the receivers to the master processing station. The bandwidth requirements of a GPS network can be a major limitation in implementing a network-based kinematic positioning system (Radovanovic, 2002). When dual-frequency receivers are used to collect GPS data, an effective way to reduce the bandwidth requirements is to combine the two carrier signals measured on the L1 and L2 frequencies, into a single combined carrier signal. In this way, it is possible to draw on the advantages of having two signals, while avoiding the problems of large bandwidth constraints.

The properties of the various combined signals vary greatly. The two most important properties of the resulting combined signals are the achievable positioning accuracy and the ease with which integer ambiguities can be resolved successfully. Some combinations, such as the widelane, make integer ambiguity resolution very successful, but the resulting positioning accuracy is quite poor. On the other hand, some combinations provide excellent positioning accuracy in fixed mode, but fixing the ambiguities to the correct integer value may be unreliable.

This paper will investigate certain linear data combinations by applying the theory of error propagation for combined signals and showing the results of both simulated and real tests.

3 Linear Combinations of Signals

A linear combination of signals is created through the application of the following equation.

$$\Phi_* = \begin{bmatrix} a & b \end{bmatrix} \begin{bmatrix} \Phi_{L1} \\ \Phi_{L2} \end{bmatrix} \quad (1)$$

where Φ_* is the carrier phase measurement of the combined signal, a and b are the combination coefficients, and Φ_{L1} and Φ_{L2} are the original carrier phase observations at the L1 and L2 frequencies, respectively. In order to preserve the integer nature of the ambiguities, the coefficients, a and b must be integers as well.

Applying the covariance law to Eq. (1) for the case of double differences, the measurement accuracy in units of cycles² can be calculated as follows:

$$\begin{aligned} \nabla\Delta\mathbf{s}_*^2 = & \left(\frac{\partial\Phi_*}{\partial\Phi_{L1}}\right)^T \nabla\Delta\mathbf{s}_{\Phi_{L1}}^2 \left(\frac{\partial\Phi_*}{\partial\Phi_{L1}}\right) + \left(\frac{\partial\Phi_*}{\partial\Phi_{L1}}\right)^T \nabla\Delta\mathbf{s}_{\Phi_{L1}\Phi_{L2}}^2 \left(\frac{\partial\Phi_*}{\partial\Phi_{L2}}\right) + \\ & + \left(\frac{\partial\Phi_*}{\partial\Phi_{L2}}\right)^T \nabla\Delta\mathbf{s}_{\Phi_{L2}\Phi_{L1}}^2 \left(\frac{\partial\Phi_*}{\partial\Phi_{L1}}\right) + \left(\frac{\partial\Phi_*}{\partial\Phi_{L2}}\right)^T \nabla\Delta\mathbf{s}_{\Phi_{L2}}^2 \left(\frac{\partial\Phi_*}{\partial\Phi_{L2}}\right) \end{aligned} \quad (2)$$

where $\nabla\Delta\mathbf{s}_\Phi^2$ represents the variance of the indicated double difference measurement in units of cycles². The quantities, $\nabla\Delta\mathbf{s}_{\Phi_{L1}\Phi_{L2}}$ and $\nabla\Delta\mathbf{s}_{\Phi_{L2}\Phi_{L1}}$ are equal and describe the errors that are correlated between the L1 and L2 frequencies, namely the ionospheric and tropospheric errors. Eq. (2) can be simplified to

$$\nabla\Delta\mathbf{s}_*^2 = a^2\nabla\Delta\mathbf{s}_{\Phi_{L1}}^2 + 2ab\nabla\Delta\mathbf{s}_{\Phi_{L1}\Phi_{L2}}^2 + b^2\nabla\Delta\mathbf{s}_{\Phi_{L2}}^2. \quad (3)$$

To apply Eq. (3), all the terms must be expressed in the same units. This conversion and the resulting equations have been developed by Radovanovic et al (2001) and are repeated here for clarity.

$$\nabla\Delta\mathbf{s}_{\Phi_{L1}}^2 = \nabla\Delta\mathbf{s}_n^2 + \frac{\nabla\Delta\mathbf{s}_T^2}{I_{L1}^2} + I_{L1}^2\nabla\Delta\mathbf{s}_I^2 \quad (4)$$

$$\nabla\Delta\mathbf{s}_{\Phi_{L1}\Phi_{L2}}^2 = \frac{\nabla\Delta\mathbf{s}_T^2}{I_{L1}I_{L2}} + I_{L1}I_{L2}\nabla\Delta\mathbf{s}_I^2 \quad (5)$$

$$\nabla\Delta\mathbf{s}_{\Phi_{L2}}^2 = \nabla\Delta\mathbf{s}_n^2 + \frac{\nabla\Delta\mathbf{s}_T^2}{I_{L2}^2} + I_{L2}^2\nabla\Delta\mathbf{s}_I^2 \quad (6)$$

where I_{L1} and I_{L2} are the wavelengths of the L1 and L2 signals, $\nabla\Delta\mathbf{s}_n^2$ is the measurement variance due to receiver noise and multipath in cycles², $\nabla\Delta\mathbf{s}_T^2$ is the measurement variance due to orbital errors and the troposphere in meters², and $\nabla\Delta\mathbf{s}_I^2$ is the measurement variance due to the ionosphere in TEC/meter². By substituting Eqs. (4), (5), and (6) into Eq. (3) and rearranging terms, the following equation results.

$$\nabla\Delta\mathbf{s}_*^2 = \left[\nabla\Delta\mathbf{s}_n^2 \quad \nabla\Delta\mathbf{s}_T^2 \quad \nabla\Delta\mathbf{s}_I^2 \right] \cdot \begin{bmatrix} \frac{a^2 + b^2}{I_{L1}^2} + \frac{2ab}{I_{L1}I_{L2}} + \frac{b^2}{I_{L2}^2} \\ a^2 I_{L1}^2 + 2ab I_{L1} I_{L2} + b^2 I_{L2}^2 \end{bmatrix} \quad (7)$$

This equation shows that the accuracy of the combined signal in cycles² depends on the accuracy components of the two original carrier frequencies and the choice of coefficients, a and b . For a given GPS positioning campaign, different choices of a and b will yield vastly different accuracies. The ionosphere-free combination, $[a \ b] = \left[1 \quad -\frac{I_{L1}}{I_{L2}} \right]$, eliminates the influence of the ionosphere ($\nabla\Delta\mathbf{s}_I^2$), the troposphere-free combination, $[a \ b] = \left[1 \quad -\frac{I_{L2}}{I_{L1}} \right]$, eliminates the influence of the troposphere ($\nabla\Delta\mathbf{s}_T^2$), and the pure L1 carrier signal, $[a \ b] = [1 \ 0]$ minimizes the effect of receiver noise ($\nabla\Delta\mathbf{s}_n^2$). Other linear combinations of signals exhibit varying degrees of error mitigation.

One way to examine the degree to which the various data combinations mitigate error sources is to compare the ratio of b to a . The closer this ratio is to the ionosphere-free ratio, the less effect the ionosphere will have on the measurement. Similarly, the closer this ratio is to the ratio of the troposphere-free combination, the less affected by the troposphere the combination will be (Radovanovic et al, 2001). Table 1 lists the ratio values for various combinations.

Table 1: Ratio of $b:a$ for various data combinations

Combination	a	b	Ratio (b/a)	Wavelength (m)
Ionosphere-free	1	$-\frac{I_{L1}}{I_{L2}}$	-0.78	0.48
Troposphere-free	1	$-\frac{I_{L2}}{I_{L1}}$	-1.28	-
L1 only	1	0	0	0.19
Widelane	1	-1	-1.00	0.86
Narrowlane	1	1	1.00	0.11
-	4	-3	-0.75	0.11
-	3	-2	-0.66	0.13
-	2	-1	-0.5	0.15

It is important to note that the preceding analysis deals with the variance of measurements in units of cycles². Minimizing an error source in cycles² may not necessarily minimize the error source in units of meters². Thus, the crucial evaluation of the various data sources lies in the position domain.

4 Position Domain

The ultimate motivation behind a choice of values for a and b is to maximize the attainable positioning accuracy. In terms of least squares estimation mathematics, the positioning accuracy is calculated from a subset of the diagonal elements of the normal matrix, which can be expressed as:

$$\mathbf{N}_{total} = \mathbf{A}^T (\mathbf{B} \mathbf{C}_l \mathbf{B}^T) \mathbf{A} = \begin{bmatrix} \mathbf{N}_{par} & \mathbf{N}_{par,amb} \\ \mathbf{N}_{amb,par} & \mathbf{N}_{amb} \end{bmatrix} \quad (8)$$

where \mathbf{N}_{total} is the normal matrix, \mathbf{N}_{par} is the normal matrix for the parameters, \mathbf{N}_{amb} is the normal matrix for the ambiguities, $\mathbf{N}_{par,amb}$ is the cross-covariance matrix describing the correlations between the ambiguities and the parameters, \mathbf{A} is the design matrix with respect to the parameters, \mathbf{B} is the design matrix with respect to the observations, and \mathbf{C}_l is the variance-covariance matrix of the undifferenced observations.

The average positioning accuracy (standard deviation) is calculated by,

$$\nabla \Delta \mathbf{s} = \sqrt{\sum_{i=0}^n \text{diag}(\mathbf{N}_{par})} \quad (9)$$

where n is the number of unknown station coordinates and diag refers the main diagonal of the matrix. In fixed ambiguity mode, $\mathbf{N}_{total} = \mathbf{N}_{par}$ because there is no uncertainty associated with the ambiguities.

To gauge the effects of various linear combinations on positioning accuracy, a simulation was conducted for baselines of varying length. Five minute time spans were simulated and a typical stochastic model defined in Radovanovic (2001) was implemented. Figure 1 shows the achievable positioning accuracy of various combinations for short baselines in fixed ambiguity mode.

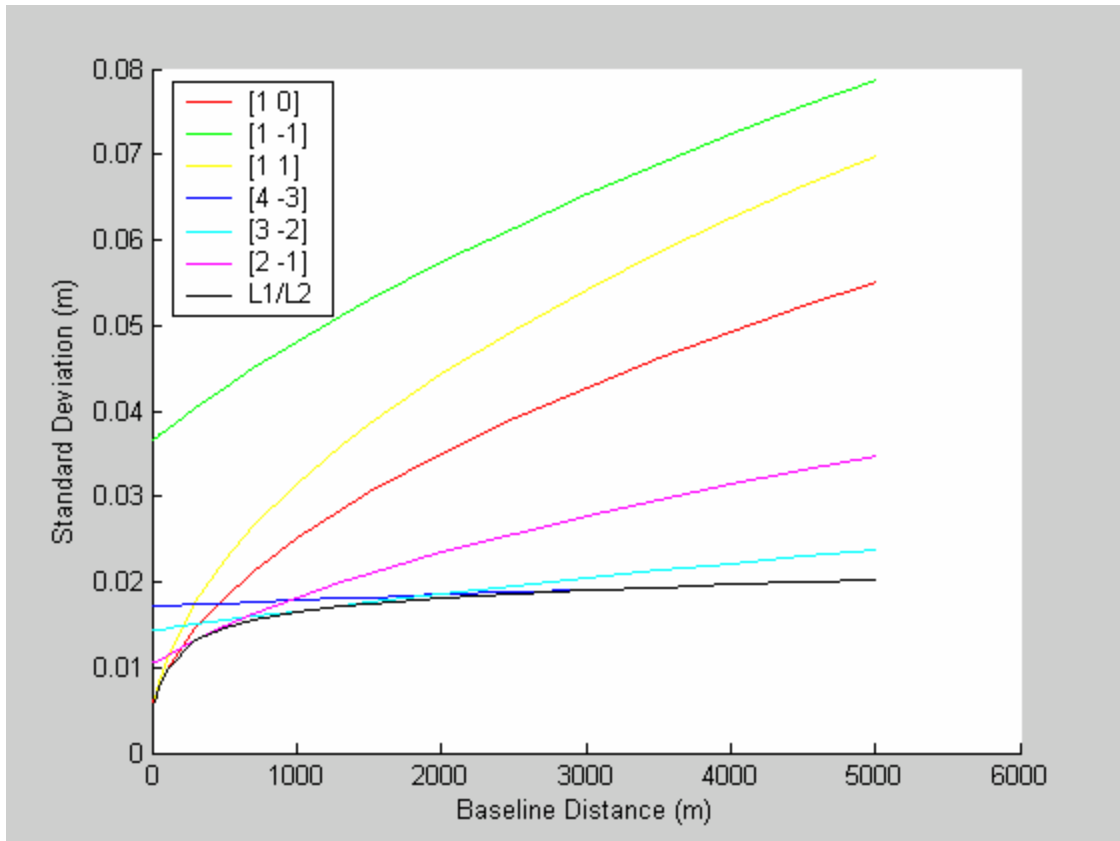


Figure 1: Positioning Accuracy of Various Data Combinations in Fixed Mode

As expected, the dual-frequency data (the black line in Figure 1) provides the best positioning accuracy. This is because when both frequencies are utilized in the solution, the frequency correlated errors are minimized and the receiver noise is not amplified.

For very short baselines (less than 200 meters), the dominant error source is the receiver noise. Therefore, the combination resulting in the smallest position error is the one that minimizes receiver noise in units of meters². However, as the baseline length increases, the ionosphere becomes the dominant error source and the combination with the smallest position error is the one that minimizes the ionospheric effect in units of meters². Of the combinations tested, the $[4 -3]$ combination has the greatest accuracy for longer baselines; whereas, the pure L1 signal (denoted as a combination with coefficients, $[1 0]$) has the greatest accuracy for short baselines. Moreover, the $[4 -3]$ combination achieves position accuracy comparable to using both L1 and L2 frequencies independently.

To verify the results of the above simulation, real data from two test networks was processed using the PADRES-GPSTM processing software (Radovanovic, 2002), which allows data to be processed using any specified linear combination. The first test network consisted of three receivers separated by 15 meters and the second network consisted of three receivers separated by 20 kilometers. In both cases, one receiver was considered to

be “roving” while the other two receivers acted as reference stations. Data was processed in a kinematic mode and the resulting position estimates were compared to the known static position of the “roving” receiver. In order to ensure the ambiguities were fixed correctly, dual-frequency measurements were used to initially solve the correct integer values of the ambiguities.

Figure 2 shows the predicted or *a posteriori* standard deviation and the real standard deviation for the short (15 meter) baseline data set. Figure 3 shows the corresponding results when the longer baseline data set is considered.

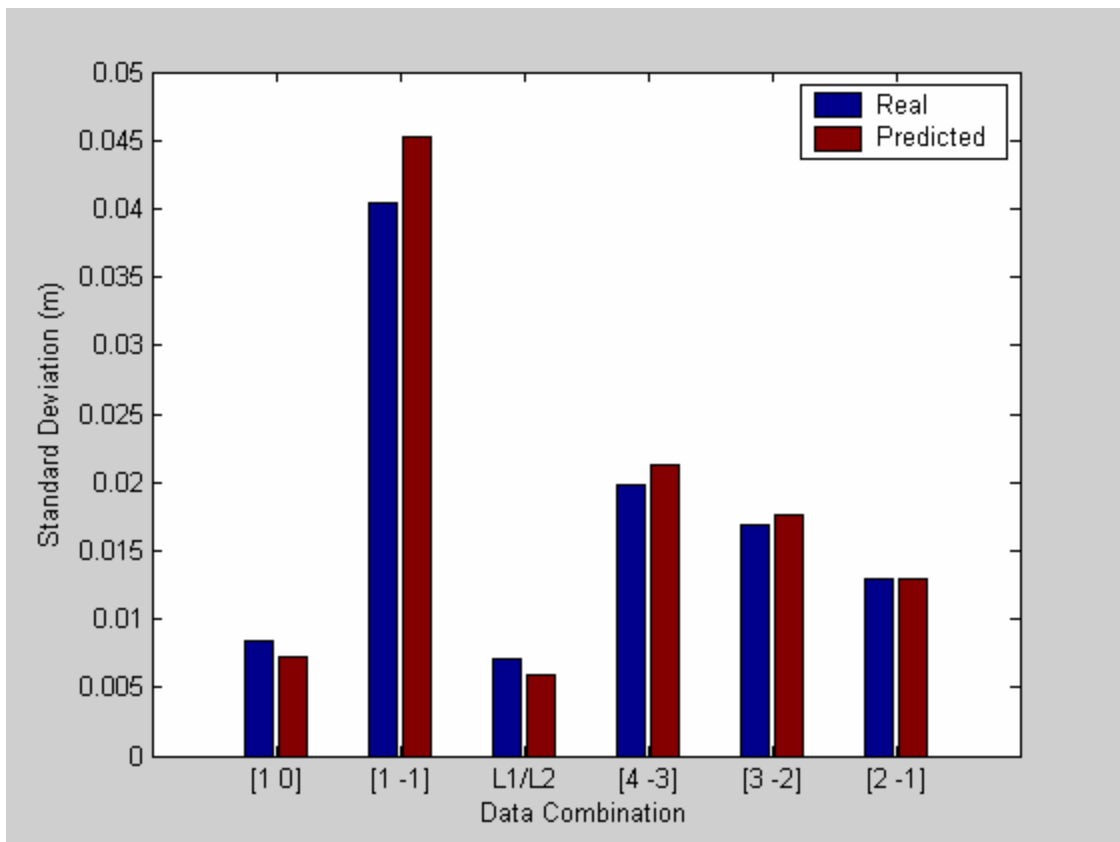


Figure 2: Position Accuracy for 15 Meter Baseline Using Real Data

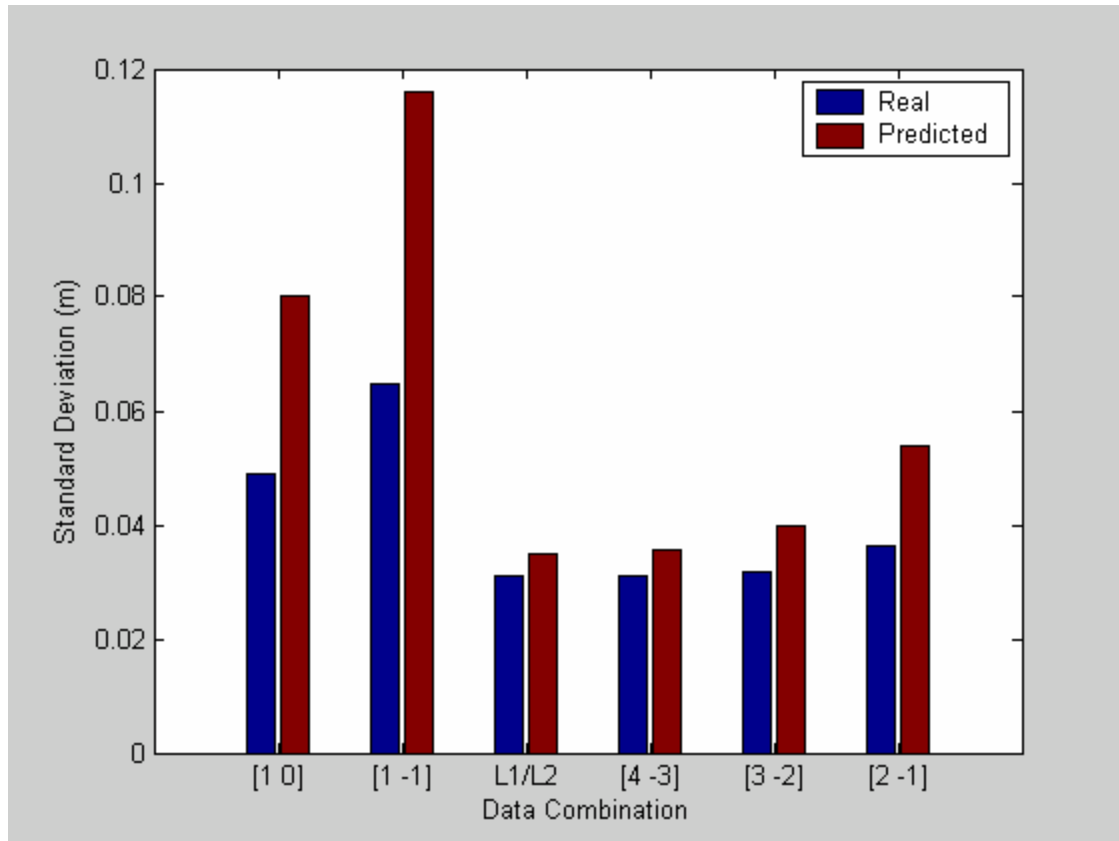


Figure 3: Position Accuracy for a 3 Receiver Network (20 km Extent) Using Real Data

The results in Figures 2 and 3 confirm the findings from the simulation data found in Figure 1. In the short baseline case, the dual-frequency solution produces the best position accuracy, the pure L1 signal delivers the best accuracy of all the data combinations, and the other combinations have significantly worse accuracies due to the amplification of receiver noise. The fact that the *a posteriori* standard deviations agree with the true position standard deviations indicates that the stochastic model used to quantify the GPS error sources is accurate for this data set.

Similarly, the longer baseline data also confirms the findings of the simulation. It is remarkable in this case that some of the combinations perform as well as if the dual-frequency measurements were used independently. Since the ionosphere is the dominant error in longer baselines, the improved performance of the [4 -3] and [3 -2] data combinations is due to the severe reduction in the effect of the ionosphere on these combined measurements. This unique property is confirmed mathematically by the similarity of the $b:a$ ratios for the [4 -3] and [3 -2] combinations to the ratio for ionosphere-free combination. Since the ratios of the [4 -3] and [3 -2] combinations are very similar to the ionosphere-free combination (see Table 1), these combinations are integer approximations of the ionosphere-free combination.

In the case of the larger extent network (Figure 3), the widelane combination and the pure L1 signal deviate significantly from the predicted standard deviations obtained from the adjustment. This divergence may indicate a discrepancy between the ionospheric error model and the true ionospheric errors. Since the widelane combination and the pure L1 signal are the most affected by ionospheric errors, the departure from reality in the model is more pronounced in these combinations.

5 Ambiguity Domain

The promising positioning accuracy of some of the aforementioned combinations (i.e. $[4 \ -3]$, $[3 \ -2]$, and $[2 \ -1]$) can be exploited only if the ambiguity values are resolved to the correct integer values. Therefore, an analysis of the likelihood of resolving the correct integer ambiguity values must be undertaken. The ability to correctly resolve integer ambiguities is directly related to the measurement accuracy in units of cycles². The measurement accuracy can be quantified by the *norm* of the $\mathbf{BC}_i\mathbf{B}^T$ term in Eq. (8). Using the same simulation data and parameters as in Section 4, the measurement accuracy has been calculated for the various data combinations and plotted in the following figure.

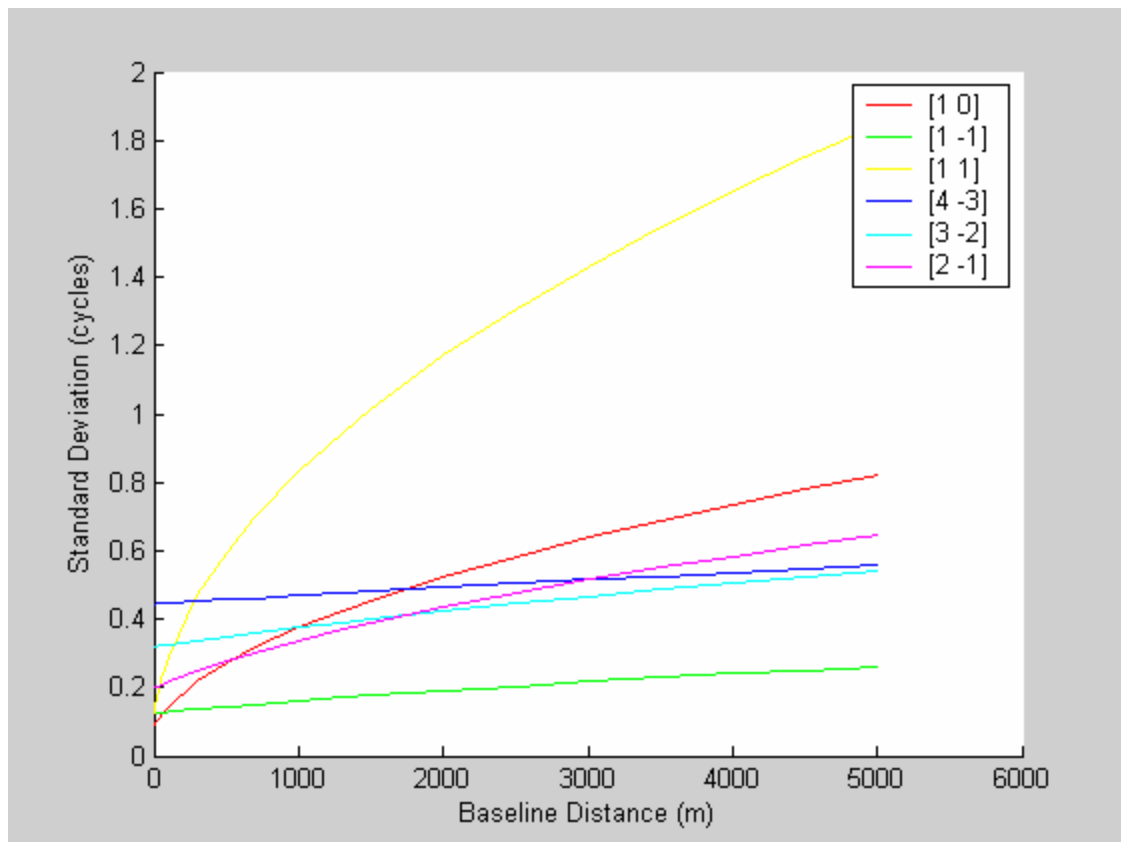


Figure 4: Measurement Accuracy of Various Data Combinations

As expected, the widelane combination (the green line in Figure 4) has the highest measurement accuracy. This is why the widelane combination provides reliable integer ambiguity resolution in practice. It is interesting to note that for longer baselines, the combinations, $[4 \ -3]$, $[3 \ -2]$, and $[2 \ -1]$ all have better measurement accuracy than the pure L1 signal. This is because of the mitigation of the ionospheric error in these combinations.

Joosten and Tiberius (2000) develop the following expression to compute the ambiguity success rate (ASR) which is the lower bound probability that the ambiguities will be estimated as the correct integer values:

$$ASR = \prod_{i=1}^n \left[2\Phi\left(\frac{1}{2\mathbf{s}_{i/I}}\right) - 1 \right] \leq P(\tilde{a} = a) \quad (10)$$

$$\Phi(x) = \int_{-\infty}^x \frac{1}{\sqrt{2\mathbf{p}}} e^{-\frac{1}{2}z^2} dz \quad (11)$$

where $\Phi(x)$ is the standard normal cumulative probability distribution, $\mathbf{s}_{i/I}$ is the standard deviation of the ambiguity, i , conditioned on all other ambiguities, \tilde{a} is the true integer value of the ambiguity, and a is the estimated integer ambiguity. This equation can be used to quantify the probability that all the ambiguities will be computed correctly. Figure 5 shows the resulting predicted success rates for various linear combinations. The stochastic error models and the simulation parameters are the same as those used previously.

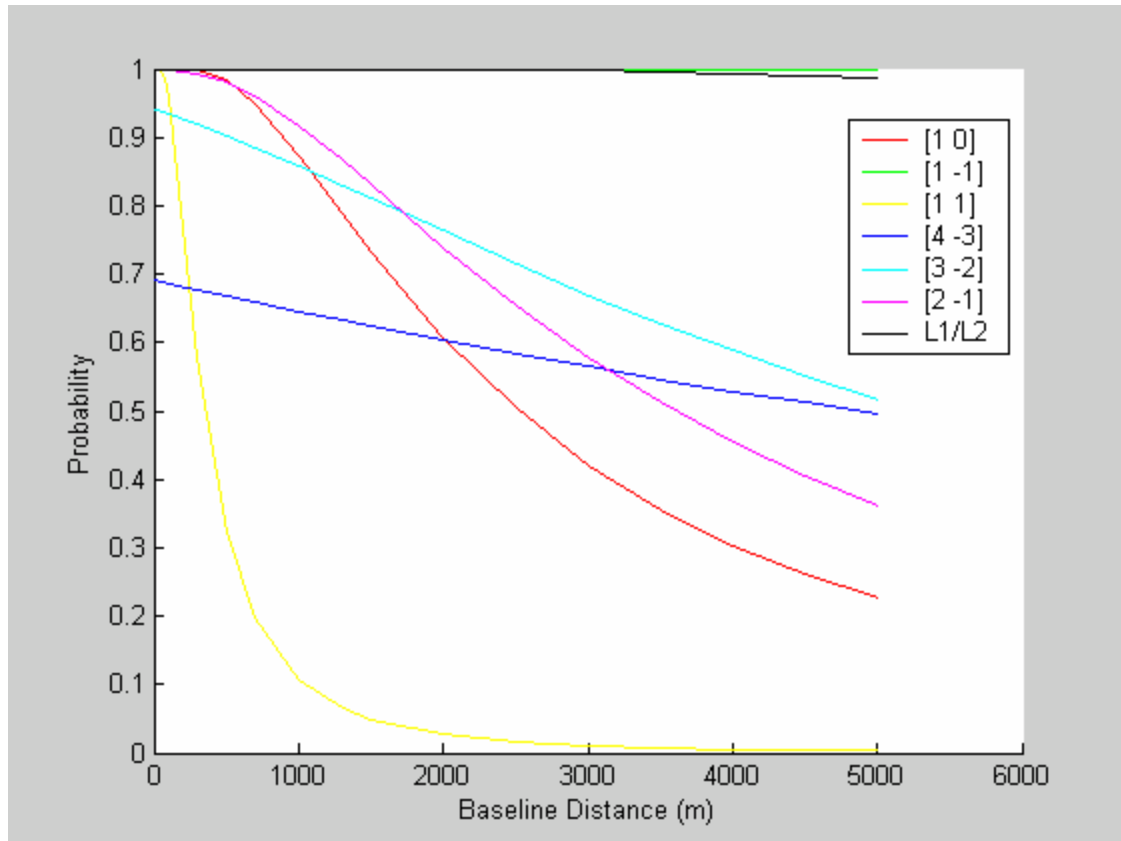


Figure 5: Probability that all Ambiguities are Resolved to the Correct Integer Value

Figures 4 and 5 support each other since the probability of fixing all ambiguities correctly is related to the measurement accuracy in unit of cycles². However, it should also be noted that for longer baselines, none of the data combinations except the widelane have sufficient ambiguity success rates to be used in practice.

Once again, the relevance of this simulation is subject to the accuracy of the stochastic error models used. Therefore, it is necessary to test the ambiguity success rate of the various combinations using real data. Two tests were performed to test the ambiguity success rate, one test involved a small three receiver network (baseline lengths from 8 to 16 meters) and the second test used a longer baseline of five kilometers. In both cases, the data was divided into independent five minute segments to simulate kinematic positioning. This technique to replicate kinematic positioning conditions enables kinematic testing, but with a known position of the static points that can be used as a truth position.

First, each time segment was processed using dual-frequency measurements with known position constraints to compute the true ambiguity values. To ensure that these values were correct, the data was processed again using the widelane combination with position constraints. The resulting ambiguities from the two cases (L1/L2 and widelane) were compared to verify that both estimations of the integer ambiguities were consistent. These ambiguity values were then accepted as the true ambiguities. The data segments were

then processed again for each data combination without position constraints to simulate a kinematic positioning campaign. Figure 6 shows the probability that all the ambiguities would be resolved to the correct integer value in a given five minute time segment. The blue bars represent the actual ambiguity success rate and the red bars represent the predicted ambiguity success rate based on Eq. (10).

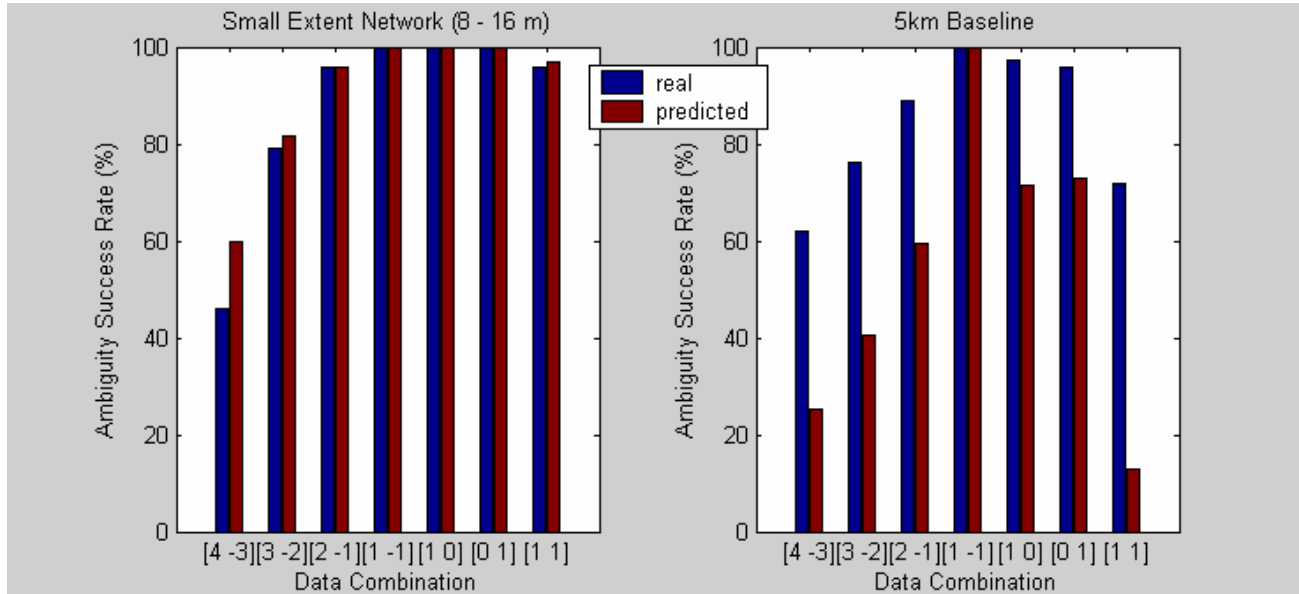


Figure 6: Ambiguity Success Rate

This figure shows that every data combination studied, with the exception of the widelane, makes ambiguity resolution less successful than using a pure L1 carrier signal. In particular, even with the small network of receivers, the ambiguity success rate for the [4 -3] combination is less than 45 percent. The reason for this disappointing result is that the variance of the receiver noise in units of cycles², which is the dominant error source for short baselines, is multiplied by a factor of 25 ($4^2 + (-3)^2 = 25$, see Eq. (7)) compared to the receiver noise level of the pure L1 signal. In the case of the longer baseline data, actual results seem to contradict the simulated ambiguity success rates. Again, this can be explained by the fact that an imperfect error model has been used in the simulation.

When comparing the ASR results from the small network to the longer baseline, it can be seen that every data combination except the [4 -3] and the widelane combinations perform poorer in terms of their ability to resolve correct integer ambiguities. This is understandable because the spatially correlated errors, especially the ionosphere, increase in magnitude as the baseline lengths increase. Hence, it is expected that the ambiguity success rates should decrease as the ionospheric measurement errors increase. The fact that the ASR of the [4 -3] combination does not get worse as the baseline length increases substantiates that this combination is very resilient to ionospheric errors as discussed in Section 4. The ASR of the widelane combination is exactly the same (100

percent) for both the small network test and the longer baseline test. Unlike the $[4 \ -3]$ combination, this constancy is not attributed to the resilience from ionospheric error of the widelane combination, but rather that the widelane has a much greater measurement precision in units of cycles². Hence, the widelane is able to fix all ambiguities correctly for both the short and long baselines.

For the longer baseline test, there are significant discrepancies between the predicted ASR and the actual ASR. This discrepancy again indicates an inadequacy of the stochastic model used for long baselines. More testing and research is required to develop a GPS error model that is suitable for all baseline lengths.

6 Position Constraints

In order to improve the ambiguity success rate performance of the various data combinations, a position constraint can be used to improve the standard deviations of the ambiguities prior to estimating the integer values. To apply a position constraint, the *a priori* knowledge about the position and the precision of this knowledge is used to improve the accuracy of the ambiguities in the normal matrix. Mathematically, this is achieved by,

$$\mathbf{N} = \mathbf{A}^T (\mathbf{B}\mathbf{C}_l\mathbf{B}^T)^{-1} + \mathbf{C}_x^{-1} \quad (12)$$

where the terms are the same as those in Eq. (8) and \mathbf{C}_x is the position constraint matrix. For the purpose of this test, a position constraint of one millimetre was used for all the station coordinates. Figure 7 shows the ambiguity success rate for the various data combinations using the position constraint.

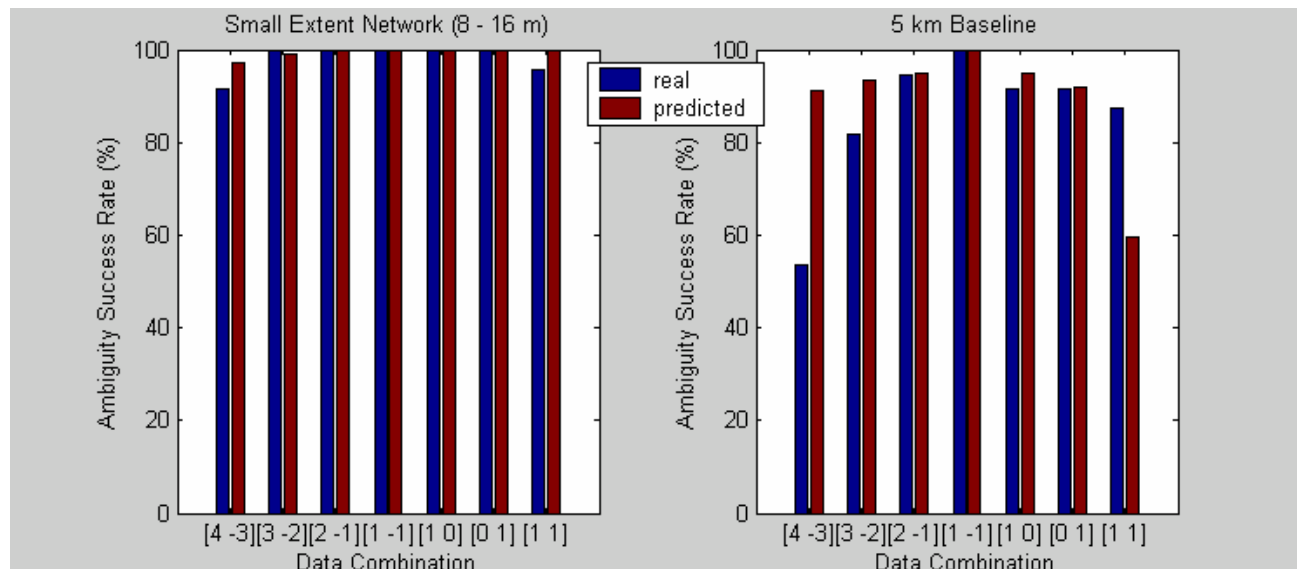


Figure 7: Ambiguity Success Rates with Position Constraints

As expected, the position constraints improve the ambiguity success rates in all cases. Using the position constraints, the ASR of all the data combinations are above 90 percent for the small extent network. However, for the longer baseline, the ASR of the $[4 \ -3]$ and $[3 \ -2]$ combinations are both below 0.85, rendering them unusable when solution reliability is critical.

7 Potential Application

The usefulness of the data combinations investigated is limited to specific applications. For example, for longer baselines (~five kilometers), the use of the $[2 \ -1]$ data combination would greatly improve positioning results when compared with the use of the pure L1 signal. According to Figure 7, the ambiguities for the $[2 \ -1]$ combination can be resolved successfully 94 percent of the time if a position constraint is applied. Once the ambiguities are resolved correctly, the positioning accuracy would be better than the accuracy achieved using the pure L1 signal (see Figure 1). Therefore, in a kinematic high precision surveying mission, a network of base receivers spaced not more than five kilometers apart could be arranged. Then after a brief initialization period at a known location to resolve the integer ambiguities, the roving receiver could move to any location within the network. All receivers would be transmitting only one signal, the combined signal, but the positioning results would be far better than the results of using the pure L1 signal. Hence, the bandwidth requirements of the network would be the same as for a single frequency network, but the attainable positioning accuracy would be improved. Certainly, the choice of an optimal data combination for any application would depend on the extent of the receiver network and the magnitudes of the GPS error components.

8 Conclusion

Many GPS networks are limited by the large bandwidths required to transmit dual-frequency data between stations. In order to combat this problem, dual-frequency measurements can be merged into an integer linear combination of signals. Certain combined signals can produce very promising results in terms of positioning accuracy. The $[4 \ -3]$ and $[3 \ -2]$ closely resemble the ionosphere-free combination and are very resilient to ionospheric errors in longer baseline scenarios. However, for short baselines, the amplification of receiver noise and multipath errors causes these combinations to perform worse than the pure L1 signal.

In order to capitalize on the achievable positioning accuracy of the combined signal, the unknown ambiguities must be resolved to their correct integer values. To evaluate the ability to resolve ambiguities, simulated and real data were used for each of the studied data combinations. For longer baselines in which the dominant measurement error is the ionosphere, the model used for representing the GPS errors breaks down, resulting in

untrustworthy predictions of the ambiguity success rate. The widelane combination provides the most reliable ambiguity resolution of the combinations tested, but this combination fails to provide desirable accuracy in the position domain. Conversely, the $[4 \ -3]$ combination, gives excellent position accuracy results akin to independent dual-frequency measurements, but it is very difficult to resolve the ambiguities to the correct integer values. The other combinations result in varying degrees of position accuracy and ambiguity success rate. In all cases, if a position constraint is introduced, the ability to resolve integer ambiguities correctly improves. In practice, applying a position constraint to initially solve the integer ambiguities is a feasible way to accomplish high precision kinematic positioning.

For a five kilometer baseline, it has been found that the $[2 \ -1]$ combination provides the best performance. However, the optimal choice of data combination depends on the application. Namely, the extent of the network and the magnitude of the various error sources must be considered.

9 Future Work

Future work by the authors will include extending the analysis of data combinations to include the new GPS civilian frequency and the proposed signals from the European global navigation satellite system, GALILEO. With three or more available frequencies, more options will become available in terms of the signals to use and how to optimally combine them to reduce bandwidth requirements. In addition, the application of fuzzy logic to automate the decision of an optimal combination will be undertaken.

10 References

De Jonge, P. and C. Tiberius (1996): The LAMBDA Method for Integer Ambiguity Estimation: Implementation Aspects. *Delft Geodetic Computing Centre LGR Series No. 12*.

Han, S. and C. Rizos (1999): The Impact of Two Additional Civilian GPS Frequencies on Ambiguity Resolution Strategies. *55th National Meeting U.S. Institute of Navigation, "Navigational Technology for the 21st Century"*, Cambridge, Massachusetts, 28-30 June, 315-321.

Hoffmann-Wellenhof, B., H. Lichtenegger, and J. Collins (1994): *GPS Theory and Practice*, Fifth edition, Springer-Verlag.

Joosten, P. and C. Tiberius (2000): Fixing the Ambiguities: Are You Sure They're Right?, *GPS World*, May Vol. 11, No. 5, pp. 46-51.

Krakiwsky, E. (1990): *The Method of Least Squares: A Synthesis of Advances. (Lecture Notes) Geomatics Engineering Department, University of Calgary, ECGE Report Number 10003. The University of Calgary, Calgary, Canada.*

Radovanovic, R. and N. El-Sheimy (2002): *Using Optimal GNSS Multi-Frequency Carrier Phase Combinations for Precise Kinematic Positioning. Presented at the ION 58th Annual Meeting 2002. Albuquerque, New Mexico. July 2002.*

Radovanovic, R. (2002): [Adjustment of Satellite-Based Ranging Observations for Precise Positioning and Deformation Monitoring](#), *UCGE Report No. 20166*. Ph.D. Dissertation. The University of Calgary, Calgary, Canada.

Radovanovic, R., G. Fotopoulos, N. El-Sheimy. (2001): *On Optimizing GNSS Multi-Frequency Carrier Phase Combinations for Precise Positioning. Presented at the IAG 2001 Scientific Assembly, Budapest, Hungary. Sept. 2-7, 2001.*